



SiPMs in Direct ToF Ranging Applications

This white paper is intended to assist in the development of SiPM (Silicon Photomultiplier) based LiDAR (Light Detection and Ranging) systems. The following sections contain information on the design and implementation of a direct ToF (Time-of-Flight) rangefinder, in terms of the laser, timing and optical parameters and detailed analysis of key aspects that must be considered when integrating SiPMs in such systems.

SiPMs in Direct ToF Ranging Applications

Introduction

LiDAR is a ranging technique that is increasingly being employed in applications such as mobile range finding, automotive ADAS (Advanced Driver Assistance Systems), gesture recognition and 3D mapping. Employing an SiPM as the photosensor has a number of advantages over alternative sensor technologies such as APD, PIN diode and PMT particularly for mobile and high volume products. **onsemi** SiPMs can offer:

- Single Photon detection from 250 nm to 1100 nm
 - Low voltage – easy to implement system requirements
 - Low power – lower operating voltages and simple readout electronics allow a low power design
 - High bandwidth and fast response time – minimize range measurement time
 - Ability to take advantage of low laser power direct ToF ranging techniques
 - Low noise and high gain – good signal to noise ratio (SNR) is achievable
 - Standard CMOS fabrication process – low cost, highly uniform and scalable production
 - Small size SMT packaging – 1 mm sensors available
- Transitioning to SiPM sensor technology presents a different set of constraints when compared to other sensors. This white paper is intended to help the user maximise the benefits of the technology and achieve a working set-up with SiPM sensors as quickly as possible. To this end, **onsemi** has created three tools to aid the user; a MATLAB ranging model for simulation purposes, a Ranging Demonstrator hardware set-up and this document.

- A detailed MATLAB model of a direct ToF system has been created to facilitate the simulation of an SiPM-based ranging application. The model can be used to support ranging system design and may be modified to simulate a wide variety of applications and implementations.
- A SiPM-based LiDAR demonstrator system was built. Measurements were taken with this ‘Gen1’ system and used to validate the simulation results from the MATLAB model.
- This document is intended to assist the new user in the development of SiPM-based, direct ToF ranging systems. It addresses the impact of the various system and environmental factors on the resulting signal to noise ratio.

Design of a Direct ToF Ranging System

The basic components required for a direct ToF ranging system, as illustrated in Figure 1, are:

1. A pulsed laser with collimation optics
2. A sensor with detection optics
3. Timing and data processing electronics

This document focuses on system design of the laser, sensor, readout and application environment. The single-point, direct ToF baseline work performed in this white paper may be extended to more complex scanning and imaging systems.

In the direct ToF technique, a periodic laser pulse is directed at the target, typically with eye-safe power and wavelength in the infrared region. The target diffuses and reflects the laser photons and some of the photons are reflected back towards the sensor. The sensor converts the detected laser photons (and some detected photons due to noise) to electrical signals that are then timestamped by the timing electronics. This *time of flight*, t , can be used to calculate the *distance*, D , to the target from the equation $D=c\Delta t/2$, where $c = \text{speed of light}$ and $\Delta t = \text{time of flight}$. The sensor must discriminate returned laser photons from the noise (ambient light). At least one timestamp is captured per laser pulse. This is known as a single-shot measurement. The signal to noise ratio can be dramatically improved when the data from many singleshot measurements are combined to produce a ranging measurement from which the timing of

the detected laser pulses can be extracted with high precision and accuracy. Several different readout techniques exist to capture the timing information from the detected laser photon pulse, as summarized below.

Readout Techniques for Ranging

- LED (leading edge discrimination) – Involves the detection of the rising edge of a multi-photon signal. Timing accuracy is determined by the ability to discriminate the rising edge of the returned optical signal. This technique is not affected by laser pulse width.
- Full waveform digitization – The full waveform is digitized and can be over-sampled to improve accuracy. Can be difficult to implement with short laser pulses or high repetition rate sources
- TCSPC (time correlated single photon counting) – Provides the highest accuracy and greatest ambient light rejection. This technique requires that less than one signal photon is detected per laser pulse. This technique can be immune to ambient light but a short pulse duration, high repetition rate and fast timing electronics are required to achieve fast and accurate measurements.
- SPSD (single photon synchronous detection) – A form of TCSPC which provides high ambient light rejection. Electronics must be designed to deal with range ambiguity.

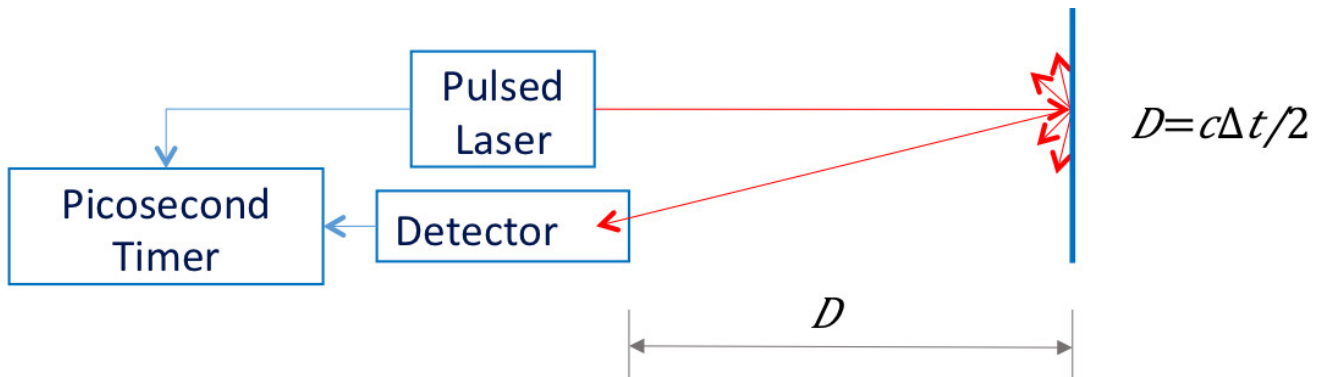


Figure 1. Direct ToF Ranging Technique Overview

Modelling A Direct ToF Ranging System

A MATLAB model of a direct ToF system has been created. A block diagram of the model is shown in Figure 2. The purpose of the model is to predict the overall performance of a system given a set of system parameters similar to those shown in Table 1.

The first step consists of analytically calculating the light levels at the sensor (both ambient and laser light) given a chosen optical scenario which can be varied by changing the corresponding system parameters. By comparing the calculated light levels to the saturation limit of the sensor, the chosen setup can be validated as suitable for ranging. In the event that the particular setup is not suitable for ranging, improvements on the setup itself can be evaluated by varying the system parameters.

The second part of the model consists of a Monte Carlo simulator where the stochastic properties of the sensor, mainly the photon detection efficiency (PDE) and the timing jitter, are reproduced. This step allows a realistic output of the sensor to be obtained by simulation. In contrast to the analytic part, this step takes into account timing information such as the acquisition time, the repetition rate of the laser and the laser pulse width. The outcome of the Monte Carlo simulation is passed to a read out model, typically a discriminator followed by a TDC (Time to Digital Converter), which produces a histogram of timestamps from which a range measurement can be extracted.

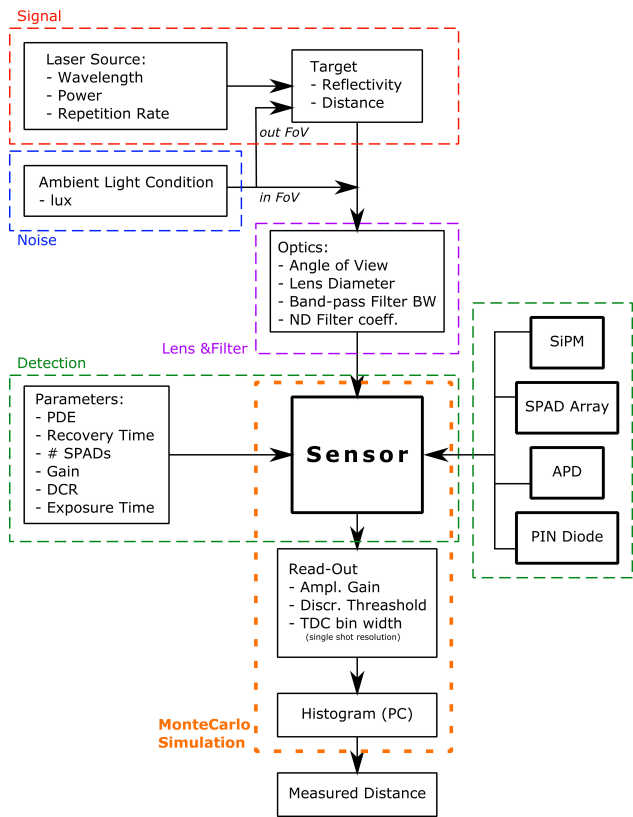


Figure 2. Calculations of Light Levels are Paired with a Monte Carlo Simulator so that a Full System Output can be Reproduced

Table 1. VARIABLES IN AN SIPM DIRECT TOF RANGING SYSTEM

| Symbol | System Parameter | Definition |
|-------------------|------------------------------------|---|
| | Acquisition method | This could be leading edge detection (LED) or time correlated single photon counting (TCSPC). |
| f | Laser repetition rate | Clock rate of the laser. This is the same as the detector single-shot rate. |
| W_{laser} | Laser pulse width | |
| λ_{laser} | Laser wavelength | Wavelength of the laser beam. |
| $FWHM_{laser}$ | Laser FWHM | Spectral FWHM of the laser beam. |
| P_{laser} | Laser peak power | Peak power of each laser pulse. |
| θ_{laser} | Laser beam divergence | The angle at which the laser beam diverges from a point source. |
| d | Laser-sensor distance | The perpendicular distance between the laser diode and the sensor limits the minimum range. Ideally this should be 0. |
| \emptyset | Collection lens aperture | A plano convex lens is placed directly in front of the sensor. Effective aperture after mounting of the lens. |
| F_{lens} | Collection lens focal length | |
| BP | Optical filter bandpass wavelength | Filter placed between sensor and collection lens. |
| $FWHM_{BP}$ | Optical filter FWHM | |
| θ_{det} | Sensor angle of view | The angle at which the field of view of the sensor diverges from a point source. |
| SiPM | SiPM | SiPM sensor. |
| A | Amplifier gain | SiPM signal amplifier. |
| V_{th} | Threshold voltage | Comparator threshold. Dictates minimum light level required to be considered an event. |
| t_{acq} | Acquisition time | The total time during which samples are recorded by the sensor for inclusion in the data. = 1/frame rate. |
| LSB_{TDC} | TDC resolution | TDC bin size limits the single-shot resolution. The use of multiple single-shot measurements can yield resolution significantly better than the TDC bin size. |
| R | Target reflectivity | |
| D | Distance to target | Distance between the ranging module and the target. |
| E_v | Ambient illuminance | The maximum illuminance on the sensor due to ambient light. |

The Ranging Histogram

Each time the laser is pulsed the acquisition system performs a single-shot measurement. Depending on many factors including the laser power and distance to the target, the number of detected laser photons per pulse may be low. Ideally, each detected photon would be timestamped. However, number of timestamps per single-shot measurement may be limited by the dead time of the TDC. Usually, many single-shot timing measurements, each containing one or more timestamps, are combined to produce a frame. The complete timing data obtained over the course of a single frame may be plotted in the form of a histogram as shown in Figure 3. The system ranging performance is limited by the quality of the histogram data, which in turn is affected by the system parameters. There are some limiting factors and some trade-offs that can be made, as can be seen from the analysis of system parameters detailed in the **The Effect of Changing System Variables Section** on page 7. The ranging histogram used below also provides a visual representation which is useful in describing the effects of various parameters on the data

obtained. The basic histogram signal and timing parameters are explained below.

The histogram signal to noise ratio, SNR_H , is the ratio of the signal peak to the maximum noise peak:

$$SNR_H = \frac{\text{Signal peak value}}{\text{Noise peak value}}$$

In the model the following terms apply to the measurement time:

$$f = \text{laser frequency}$$

The laser repetition rate limits the maximum ToF that can be measured without ambiguity and this defines the time per single-shot measurement:

$$\text{Single shot Measurement time, } t_{ss} = \frac{1}{f}$$

The frame size is the number of single-shot measurements per histogram. A larger frame size can improve SNR_H and produce a better quality histogram. The ranging speed is defined by the frame rate:

$$\text{frame rate} = \text{number of range measurements per second} = \frac{1}{t_{acq}}$$

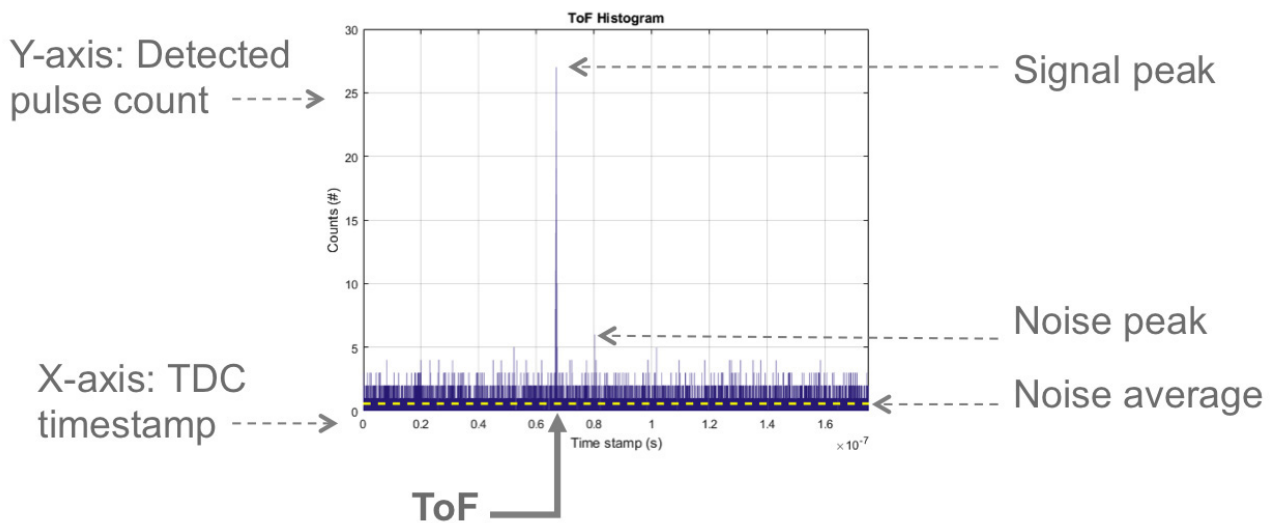


Figure 3. Histogram Example from Simulation Showing Signal, Noise and Time of Flight

The Effect of Changing System Variables

System design parameters will vary based on the requirements of a specific application. The purpose of this section is to demonstrate, using the model of a direct ToF ranging system, how the acquired data is affected by each of seven key parameters. The effect of distance to target and ambient light level are also shown. The key points are summarized in Table 2.

The histograms shown in the following sections are obtained through simulation and each histogram can be assumed to include the entire dataset obtained in a single frame. For computational speed, the histograms shown correspond to a short acquisition time.

1. Reference Histogram

Figure 4 shows the reference histogram obtained by simulation under the conditions listed in the blue call-out box on the right. This configuration is used as a reference point to show the effects of alternative system parameter values.

The system parameters used in the following analysis were chosen to provide a reference point of a typical 5 m ranging application. Some of the parameters were chosen for ease of simulation and illustrative purposes rather than to reflect an optimized setup.

In each of the following sections one parameter only is modified and the simulation re-run to illustrate the effect that parameter has on the system in terms of collected data.

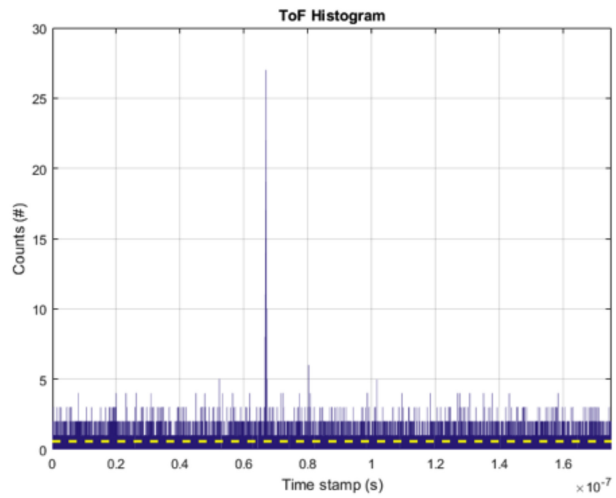


Figure 4. Reference Histogram

| | |
|------------------------------------|--------------------------------|
| $t_{acq} = 1 \text{ ms}$ | MicroFC-10020 |
| $f = 150 \text{ kHz}$ | $P_{laser} = 1 \text{ W}$ |
| $E_v = 10 \text{ klux}$ | $D = 10 \text{ m}$ |
| $\lambda_{laser} = 905 \text{ nm}$ | $W_{laser} = 250 \text{ ps}$ |
| $\varnothing = 12 \text{ mm}$ | $R = 92\%$ |
| $\theta_{det} = 1.4^\circ$ | $FWHM_{BP} = \pm 2 \text{ nm}$ |
| $SNR_H = 4.5$ | |

Table 2. SUMMARY OF EFFECTS OF KEY PARAMETERS

| Parameter | Summary | Section |
|--------------------------------|--|---------|
| Laser Source Parameters | | |
| Laser pulse repetition rate | Affects quality of data that can be collected in fixed time interval. | 2 |
| Laser pulse width | May be dictated by laser availability. Only the front edge of the laser is required for LED therefore shorter laser pulses are more efficient. | 3 |
| Laser wavelength | Optimal wavelength may be chosen in terms of solar irradiance model. | 4 |
| Sensor Parameters | | |
| Collection lens aperture | Essential that this is limited to prevent sensor saturation in high ambient light conditions. | 5 |
| Sensor angle of view | Essential that this is limited to prevent sensor saturation in high ambient light conditions. | 6 |
| Optical filter bandpass | Should be as narrow as possible to eliminate all spurious noise. | 7 |
| SiPM microcell size | Spectral range, PDE, timing and dynamic range may be optimized but choice of SiPM is secondary to other system settings. | 8 |
| Conditions | | |
| Distance to target | Dictates required laser power and achievable accuracy. | 9 |
| Ambient light | Limits achievable SNR and affects quality of data. | 10 |

2. Laser Pulse Repetition Rate

A higher laser pulse repetition rate improves the quality of the histogram by increasing the number of single-shot measurements allowing more returned laser photons to be detected for a given acquisition time. The maximum noise peak also increases as more noise counts are acquired. But, because the noise is not correlated, overall SNR_H increases, as shown in Figure 5.

There is an upper limit on the maximum laser repetition rate that may be chosen because the rate limits the distance to target that may be ranged without ambiguity. For example, if 300 m is the maximum ranging target distance then a maximum repetition rate of 1 MHz can be used. If 100 m is the maximum target distance then 3 MHz may be used.

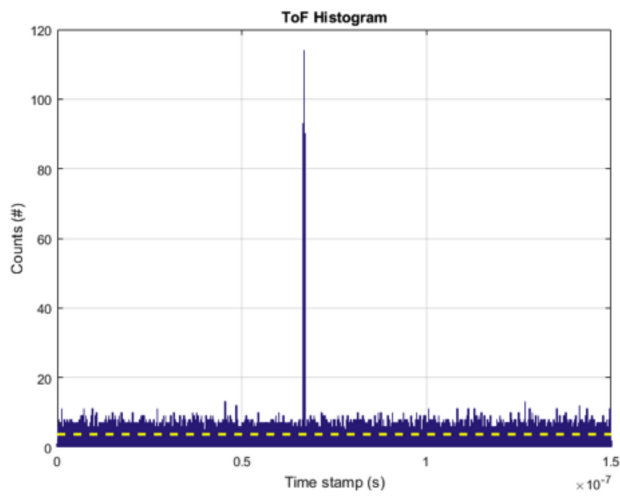


Figure 5. Effect of Laser Repetition Rate

| | |
|------------------------------------|--------------------------------|
| $t_{acq} = 1 \text{ ms}$ | MicroFC-10020 |
| $f = 1 \text{ MHz}$ | $P_{laser} = 1 \text{ W}$ |
| $E_v = 10 \text{ klux}$ | $D = 10 \text{ m}$ |
| $\lambda_{laser} = 905 \text{ nm}$ | $W_{laser} = 250 \text{ ps}$ |
| $\varnothing = 12 \text{ mm}$ | $R = 92\%$ |
| $\theta_{det} = 1.4^\circ$ | $FWHM_{BP} = \pm 2 \text{ nm}$ |
| $SNR_H = 10.5$ | |

3. Laser Pulse Width

A wider laser pulse width leads to a wider signal peak in the histogram, as shown in Figure 6. With a square pulse it is necessary to discriminate the leading edge of the pulse to locate only the time of flight of the first photons detected. Subsequent photons do not carry useful ToF information. For this reason shorter laser pulses are optimal. However the availability of suitable lasers may be the deciding factor in a practical setup.

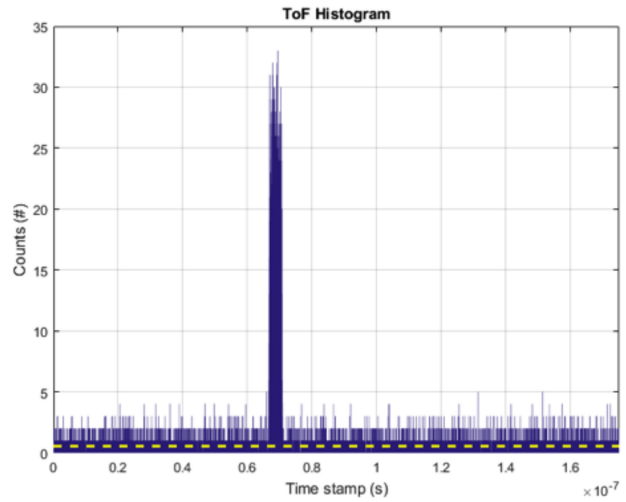


Figure 6. Effect of Wider Laser Pulse Width

| | |
|------------------------------------|--------------------------------|
| $t_{acq} = 1 \text{ ms}$ | MicroFC-10020 |
| $f = 150 \text{ kHz}$ | $P_{laser} = 1 \text{ W}$ |
| $E_v = 10 \text{ klux}$ | $D = 10 \text{ m}$ |
| $\lambda_{laser} = 905 \text{ nm}$ | $W_{laser} = 4 \text{ ns}$ |
| $\varnothing = 12 \text{ mm}$ | $R = 92\%$ |
| $\theta_{det} = 1.4^\circ$ | $FWHM_{BP} = \pm 2 \text{ nm}$ |
| $SNR_H = 6.2$ | |

4. Laser Wavelength

Selection of the laser wavelength is influenced by a number of factors including eye safety and availability of low cost lasers at particular wavelengths. Laser wavelength selection also influences ranging performance due to solar irradiance and sensor detection efficiency at different wavelengths.

For a system subject to solar noise, a longer wavelength may be chosen to exploit the corresponding reduction in solar irradiance at the longer wavelength. The effect can be seen from the model of solar irradiance in Figure 8.

With a laser wavelength of 940 nm, the PDE of the modelled SiPM is reduced from ~1% to ~0.3%. Keeping all other parameters constant, the detection efficiency of both the laser photons and ambient light photons is reduced. For this particular setup the net effect is a reduction in SNR_H due to lower total counts, as shown in Figure 7. Of course, if another SiPM were chosen that has improved PDE at the wavelength of interest, the resulting histogram signal count would be higher and SNR_H would be improved. Similarly, other parameters may be modified to compensate for the reduced PDE.

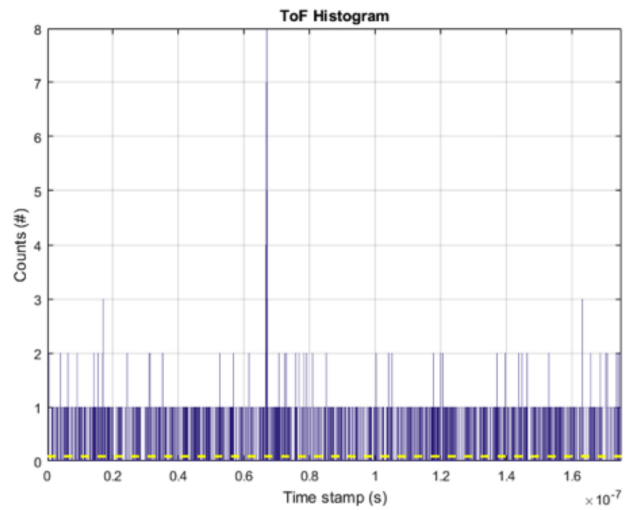


Figure 7. Effect of Increased Wavelength on Histogram

| | |
|------------------------------------|--------------------------------|
| $t_{acq} = 1 \text{ ms}$ | MicroFC-10020 |
| $f = 150 \text{ kHz}$ | $P_{laser} = 1 \text{ W}$ |
| $E_v = 10 \text{ klux}$ | $D = 10 \text{ m}$ |
| $\lambda_{laser} = 940 \text{ nm}$ | $W_{laser} = 250 \text{ ps}$ |
| $\varnothing = 12 \text{ mm}$ | $R = 92\%$ |
| $\theta_{det} = 1.4^\circ$ | $FWHM_{BP} = \pm 2 \text{ nm}$ |
| $SNR_H = 2.7$ | |

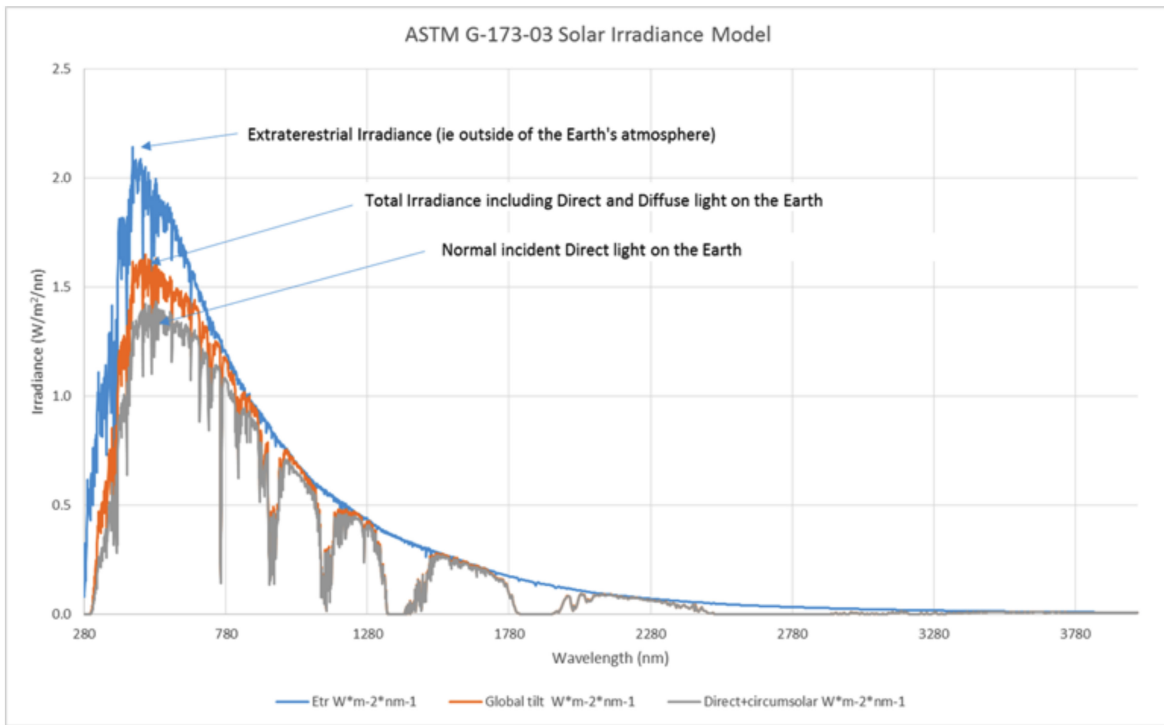


Figure 8. Solar Irradiance Model

5. Collection Lens Aperture

When the lens aperture is widened, more ambient photons are detected while the number of returned laser photons remains constant.

The SiPM is now prone to saturation as is evident from the large overshoot at the start of the histogram window in Figure 9. When the sensor is saturated the laser photons can no longer be detected by the SiPM, leading to a lower signal detection rate and lower overall SNR_H .

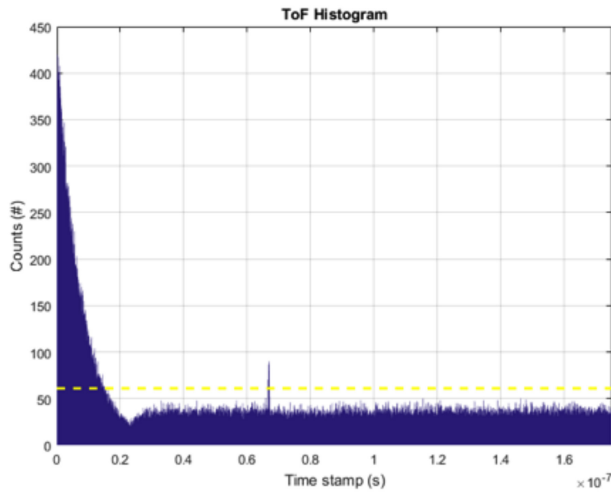


Figure 9. Effect of Increased Collection Lens Aperture

| | |
|------------------------------------|--------------------------------|
| $t_{acq} = 1 \text{ ms}$ | MicroFC-10020 |
| $f = 150 \text{ kHz}$ | $P_{laser} = 1 \text{ W}$ |
| $E_v = 10 \text{ klux}$ | $D = 10 \text{ m}$ |
| $\lambda_{laser} = 905 \text{ nm}$ | $W_{laser} = 250 \text{ ps}$ |
| $\varnothing = 20 \text{ cm}$ | $R = 92\%$ |
| $\theta_{det} = 1.4^\circ$ | $FWHM_{BP} = \pm 2 \text{ nm}$ |
| $SNR_H = 0.2$ | |

6. Sensor Angle of View

The sensor angle of view is determined by the sensor size and the focal length of the collection lens. When the sensor angle of view is increased to 20° , significantly more ambient light is incident on the SiPM. It then becomes saturated to the point that no laser pulses can be discerned by the system, as is the case in Figure 10.

It is crucial to limit the sensor angle of view to cover the field of the laser only and avoid this situation.

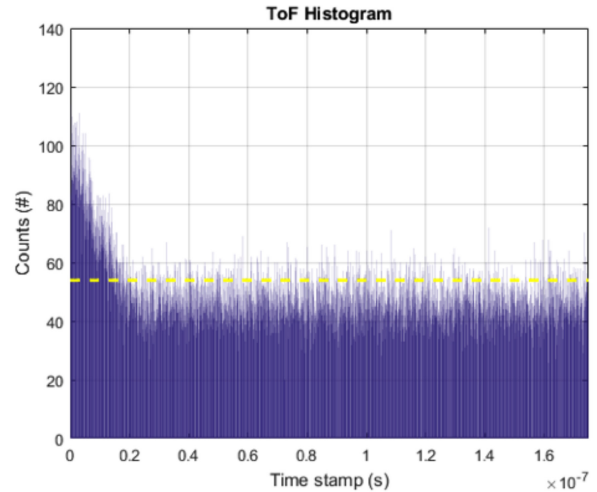


Figure 10. Effect of Increased Sensor Angle of View

| | |
|--|--------------------------------|
| $t_{acq} = 1 \text{ ms}$ | MicroFC-10020 |
| $f = 150 \text{ kHz}$ | $P_{laser} = 1 \text{ W}$ |
| $E_v = 10 \text{ klux}$ | $D = 10 \text{ m}$ |
| $\lambda_{laser} = 905 \text{ nm}$ | $W_{laser} = 250 \text{ ps}$ |
| $\varnothing = 12 \text{ mm}$ | $R = 92\%$ |
| $\theta_{det} = 20^\circ$ | $FWHM_{BP} = \pm 2 \text{ nm}$ |
| $SNR_H = (\text{no signal})$ | |

7. Optical Filter Bandpass

An optical bandpass filter is used to limit the ambient noise arising from light at wavelengths other than the laser wavelength range.

In this case the optical filter bandpass range is 50 nm FWHM (Full Width Half Maximum). This allows a wider range of wavelengths of ambient light through to the SiPM, increasing the measured background noise and worsening SNR_H as shown in Figure 11. In the model, the laser wavelength is exactly 905 nm only and the acquired laser signal is not affected by the bandpass FWHM. In real systems, the laser center wavelength may have a relatively wide variation and this may have a bearing on the choice of bandpass filter.

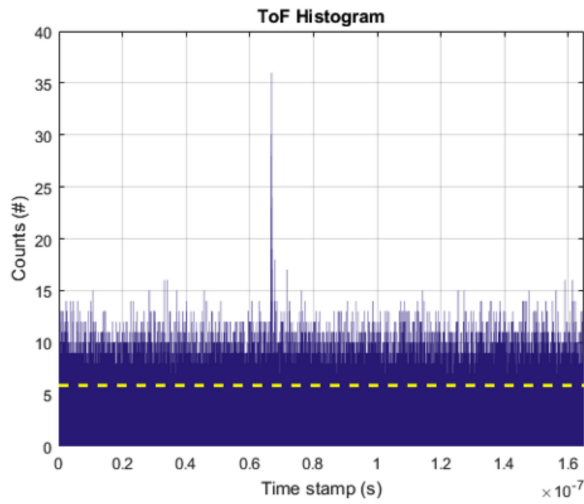


Figure 11. Effect of Wider Sensor Optical Bandpass

| | |
|------------------------------------|---------------------------------|
| $t_{acq} = 1 \text{ ms}$ | MicroFC-10020 |
| $f = 150 \text{ kHz}$ | $P_{laser} = 1 \text{ W}$ |
| $E_v = 10 \text{ klux}$ | $D = 10 \text{ m}$ |
| $\lambda_{laser} = 905 \text{ nm}$ | $W_{laser} = 250 \text{ ps}$ |
| $\varnothing = 12 \text{ mm}$ | $R = 92\%$ |
| $\theta_{det} = 1.4^\circ$ | $FWHM_{BP} = \pm 25 \text{ nm}$ |
| $SNR_H = 2.3$ | |

8. SiPM Microcell Size

The histogram in Figure 12 shows the simulated performance of a MicroFC-10035 SiPM rather than the MicroFC-10020. The main effect is the slightly increased PDE at the wavelength of interest, leading to a marginally higher signal with a smaller corresponding increase in noise. At this ranging distance and under this configuration this change of SiPM does not have a significant effect on the simulated histogram.

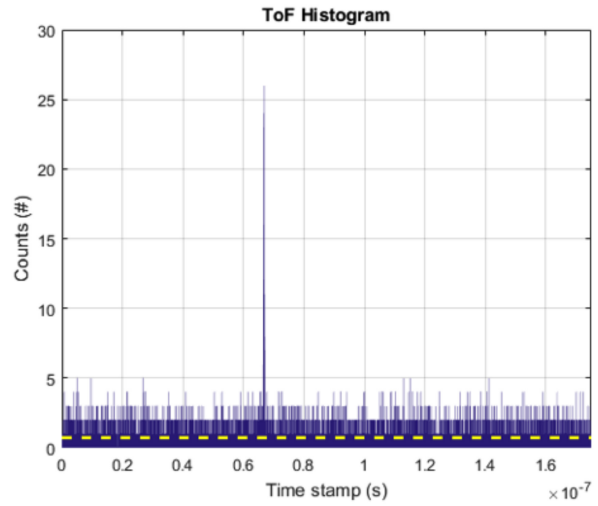


Figure 12. Effect of Changing SiPM Microcell Size

| | |
|------------------------------------|--------------------------------|
| $t_{acq} = 1 \text{ ms}$ | MicroFC-10035 |
| $f = 150 \text{ kHz}$ | $P_{laser} = 1 \text{ W}$ |
| $E_v = 10 \text{ klux}$ | $D = 10 \text{ m}$ |
| $\lambda_{laser} = 905 \text{ nm}$ | $W_{laser} = 250 \text{ ps}$ |
| $\varnothing = 12 \text{ mm}$ | $R = 92\%$ |
| $\theta_{det} = 1.4^\circ$ | $FWHM_{BP} = \pm 2 \text{ nm}$ |
| $SNR_H = 5.2$ | |

9. Distance to Target

The plot in Figure 13 superimposes histograms ranging at 10 m, 15 m, 20 m and 25 m from the target. The spacing of the signal peaks on the x-axis corresponds to $ToF = 2 \cdot distance / c$. As the distance increases the number of acquired counts from the laser is reduced because the density of laser photons at the sensor decreases with $1/d^2$ (where d is the sensor-target distance) but the ambient noise remains constant because the number of ambient photons diffused back from the target does not change with distance. At 30 m, ranging is no longer possible using this configuration. The configuration may of course be optimized to perform ranging at this distance (refer to the **Ranging Demonstrator Modelled to 100 m** Section 3 on page 15 for a setup that models ranging at long distance).

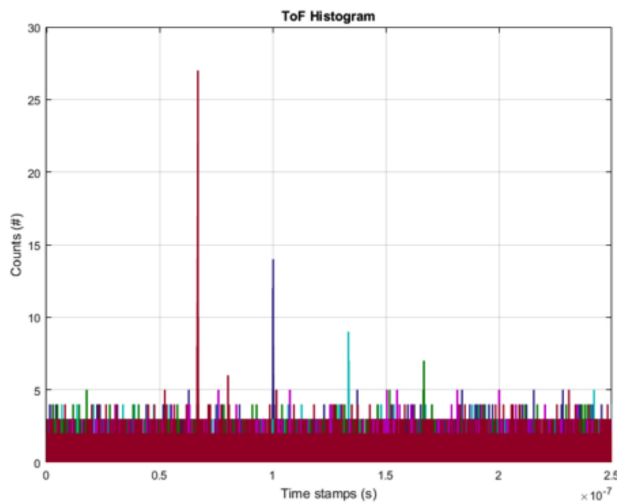


Figure 13. Effect of Increasing Target Distance

| | |
|---|---|
| $t_{acq} = 1 \text{ ms}$ | MicroFC-10020 |
| $f = 150 \text{ kHz}$ | $P_{laser} = 1 \text{ W}$ |
| $E_v = 10 \text{ klux}$ | $D = 10/15/20/25 \text{ m}$ |
| $\lambda_{laser} = 905 \text{ nm}$ | $W_{laser} = 250 \text{ ps}$ |
| $\varnothing = 12 \text{ mm}$ | $R = 92\%$ |
| $\theta_{det} = 1.4^\circ$ | $FWHM_{BP} = \pm 2 \text{ nm}$ |
| $SNR_H = 4.5/2.8/1.8/1.4$ | |

10. Ambient Light

Here the ambient light is increased 10 times to 100 klux. With an increased number of ambient photons hitting the sensor and all other conditions remaining constant, more ambient photons are acquired for every single-shot measurement. The noise counts per bin over the entire frame increases accordingly and SNR_H is negatively affected. Figure 14 shows that the peak at 10 m is still discernible and therefore ranging is still possible with this configuration at this light level, but the range capability will now be reduced.

Conversely, at low ambient light SNR_H would be improved due to lower noise counts.

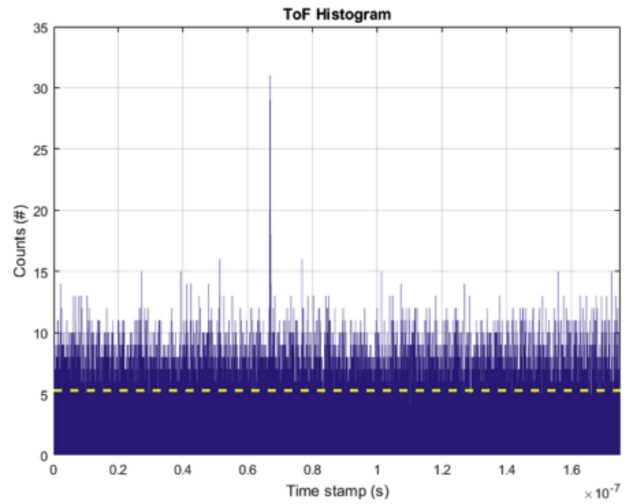


Figure 14. Effect of Increased Ambient Light

| | |
|--|--------------------------------|
| $t_{acq} = 1 \text{ ms}$ | MicroFC-10020 |
| $f = 150 \text{ kHz}$ | $P_{laser} = 1 \text{ W}$ |
| $E_v = 100 \text{ klux}$ | $D = 10 \text{ m}$ |
| $\lambda_{laser} = 905 \text{ nm}$ | $W_{laser} = 250 \text{ ps}$ |
| $\varnothing = 12 \text{ mm}$ | $R = 92\%$ |
| $\theta_{det} = 1.4^\circ$ | $FWHM_{BP} = \pm 2 \text{ nm}$ |
| $SNR_H = 1.9$ | |

The Gen1 Ranging Demonstrator Description

The Gen1 Ranging Demonstrator is an evaluation system designed to provide an introduction to direct ToF ranging using SiPM sensors. The Gen1 features:

- Optical Interface including laser collimation lens, sensor collection lens and bandpass filter
- Laser diode and driver circuit
- SiPM sensor and discriminator circuit
- FPGA-based Time-to-Digital Converter (TDC), readout and communications interface
- PC based software.

Figure 15 shows the system block diagram.

The demonstrator uses a 905 nm laser diode with a pulse width of 150 ps and a peak laser power of up to 2 W. The laser pulse repetition rate is 150 kHz. The laser output signal is collimated by a lens with a divergence of 0.06° .

At the receiver the reflected signal is focused on the sensor using a 40 mm focal length collection lens with an aperture

of 11.4 mm diameter. The sensor angle of view is 1.4° . The signal is also filtered by an optical bandpass filter with a FWHM of 10 nm.

The detection signal chain consists of a SensL MicroFC-10020-SMT SiPM, a gain stage and a high-speed comparator, which performs leading edge discrimination, and pulse generator circuit. The resulting pulses are timestamped using either a standalone TDC or an FPGA based TDC and data acquisition system. The acquired data is transferred to PC software via a high speed USB link.

The system software builds the histogram from the acquired data, which is plotted for analysis. A curve fitting algorithm extracts the ToF, as described in The Ranging Histogram Section on page 6.

Software adjustable settings allow a range of configurations to be selected in order to optimize the system for a variety of applications.

The demo is portable and is powered by a 6 V source.

A full list of the Gen1 system parameters is given in Table 3.

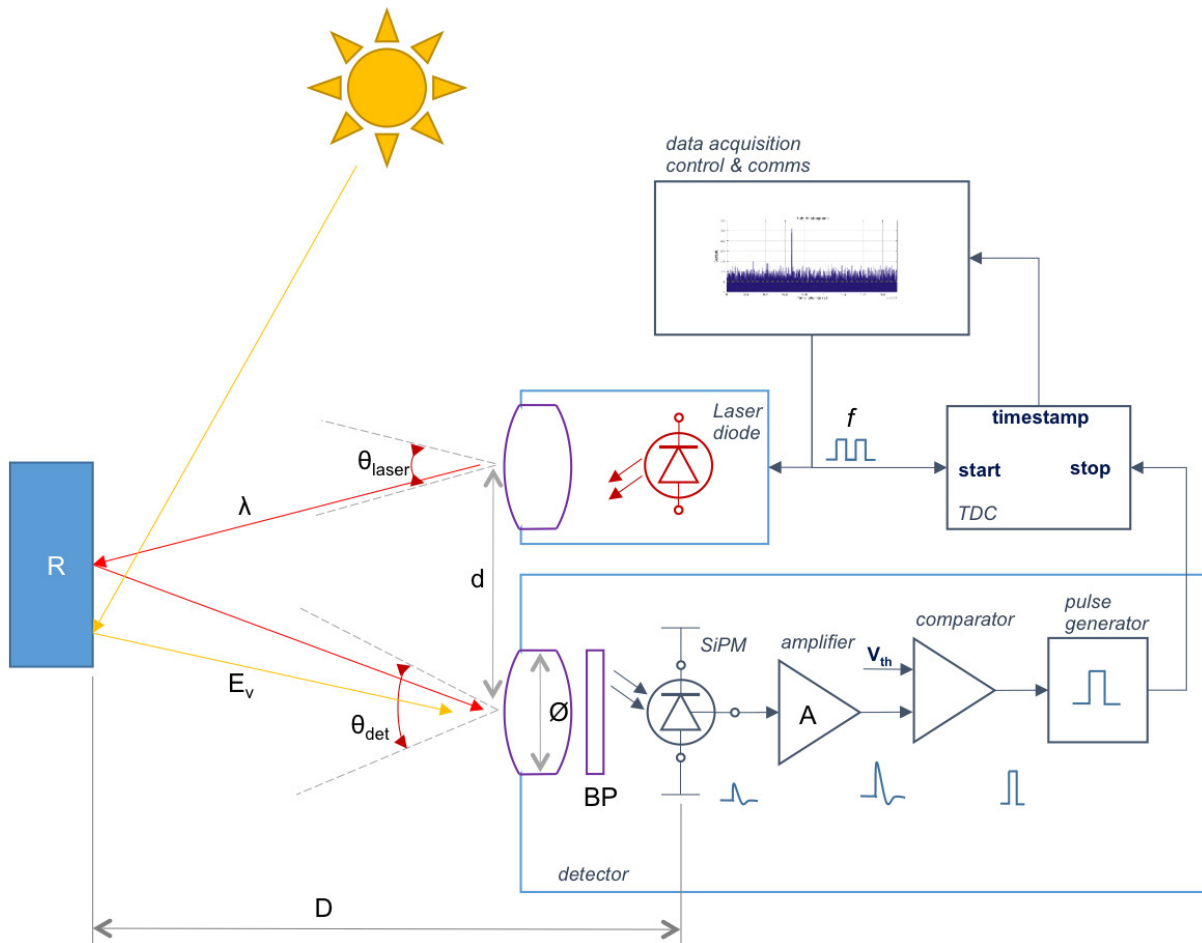


Figure 15. The Gen1 Ranging Demonstrator Schematic Block Diagram

Table 3. GEN1 SYSTEM PARAMETERS FOR SENSOR-TARGET DISTANCES UP TO 5 M

| Symbol | System Parameter | Value |
|-------------------|------------------------------------|--------------------------|
| | Acquisition method | LED |
| f | Laser repetition rate | 150 kHz |
| W_{laser} | Laser pulse width | 150 ps |
| λ_{laser} | Laser wavelength | 905 nm |
| $FWHM_{laser}$ | Laser FWHM | 7 nm |
| P_{laser} | Laser peak power | 1.39 W |
| θ_{laser} | Laser beam divergence | 0.0573° (1 mrad) |
| d | Laser-sensor distance | 2.35 m |
| \varnothing | Collection lens aperture | 11.4 mm |
| F_{lens} | Collection lens focal length | 40 mm |
| BP | Optical filter bandpass wavelength | 905 nm |
| $FWHM_{BP}$ | Optical filter FWHM | 10 nm |
| θ_{det} | Sensor angle of view | 1.4° |
| SiPM | SiPM | MicroFC-10020 |
| A | Amplifier gain | 34 dB |
| V_{th} | Threshold voltage | 40 mV |
| t_{acq} | Acquisition time | 400 ms |
| LSB_{TDC} | TDC resolution | 15.625 ps |
| R | Target reflectivity | 5% – 95% |
| D | Distance to target | 0.1 m – 5 m |
| E_v | Ambient illuminance | Office lighting: 250 lux |

1. Performance of the Gen1 Ranging Demonstrator

The performance of the Gen1 Ranging Demonstrator has been measured in a number of use cases with varying distance to target and ambient light conditions.

A summary of the actual measured ranging data from 0 m to 5 m is shown in Figure 16 in the form of a ranging data histogram, the resulting measured range vs actual range characteristic and associated range error.

Table 4 summarizes the performance of the Gen1 system up to 5 m, under lab conditions of 250 lux ambient light.

Table 4. PERFORMANCE SUMMARY FOR THE GEN1 SYSTEM UP TO 5M

| Range | 0.3 m – 0.8 m | 5 m |
|------------|---------------|-------|
| Accuracy | <3 mm | <3 mm |
| Resolution | <1 mm | <1 mm |

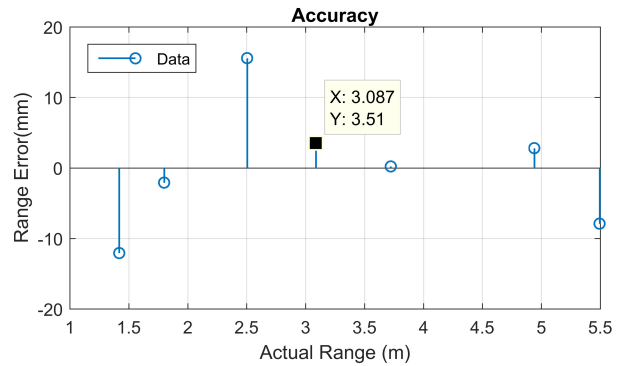
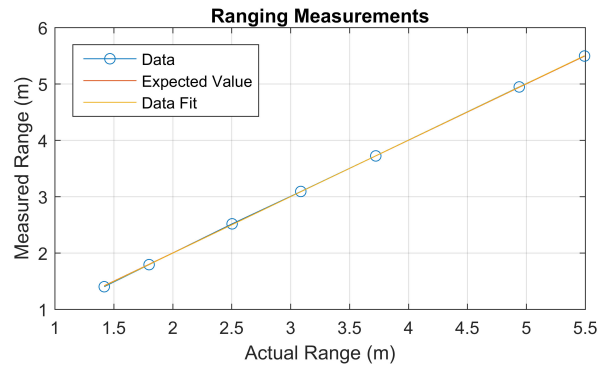
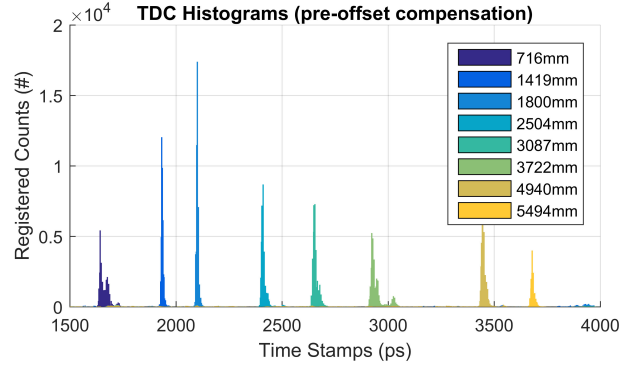


Figure 16. Baseline Performance Data from the Gen1 System up to 5 m

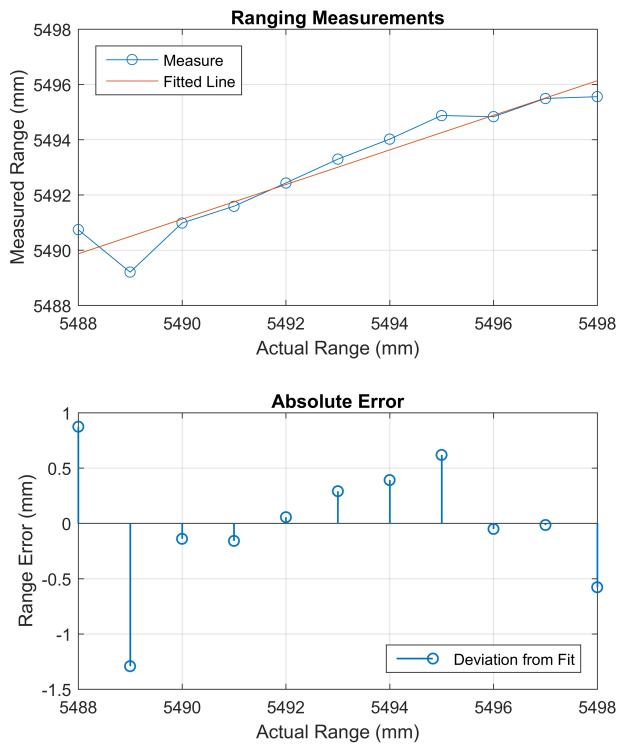


Figure 17. Data taken with the Gen1 Ranging Demonstrator

2. Validation of the Model using the Gen1 System Measurements

The model was configured with the system parameters of the demonstrator and simulated with the same distance to target and ambient light conditions. The simulated results were then compared to the measured results from the Ranging Demonstrator with good correlation as shown in Figure 17 and Figure 18. This validates the model and provides a means to design a system for different use cases.

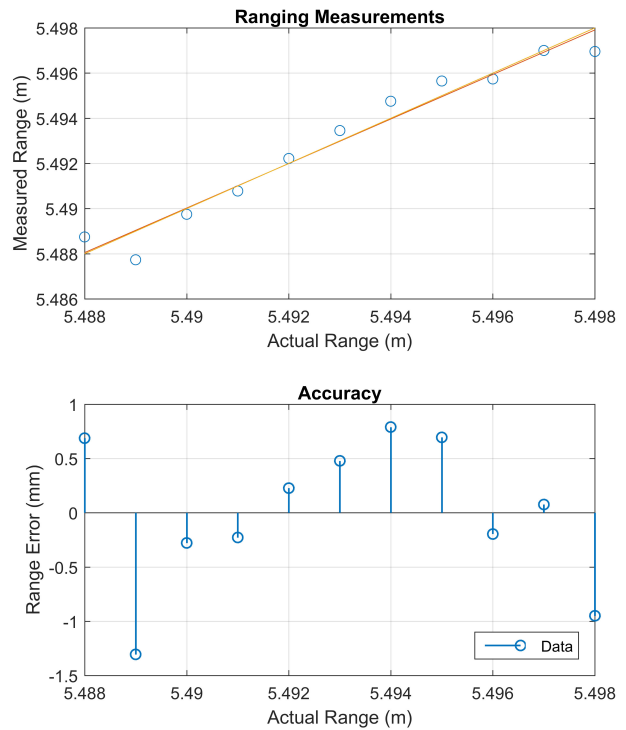


Figure 18. MA TLAB Model Simulated Data

3. Upgrading the Gen1 System to the Gen2 to 100 m

The model was then used to develop a set of system parameters that would enable Gen1 system to be upgraded to be able to achieve 100 m ranging. This system upgrade is referred to as the Gen2 system. These parameter changes are shown in Table 5. Figure 19 shows the simulated histogram, Figure 20 shows the simulated range resolution at 100 m, and Figure 21 the ranging over the full 10 m – 100 m range showing good linearity. The resulting system performance is summarized in Table 6. The Gen2 can be seen in action in this [video](#).

Table 5. SYSTEM PARAMETERS FOR THE GEN2 UPGRADED RANGING DEMONSTRATOR SYSTEM

| Parameter | Specification |
|------------------------|---------------|
| Laser peak power | 10 W |
| Laser pulse width | 667 ps |
| Ambient illuminance | 100 klux |
| Acquisition time | 100 ms |
| Optical filter FWHM | 50 nm |
| Detector Angle of View | 0.2° |
| TDC resolution | 100 ps |

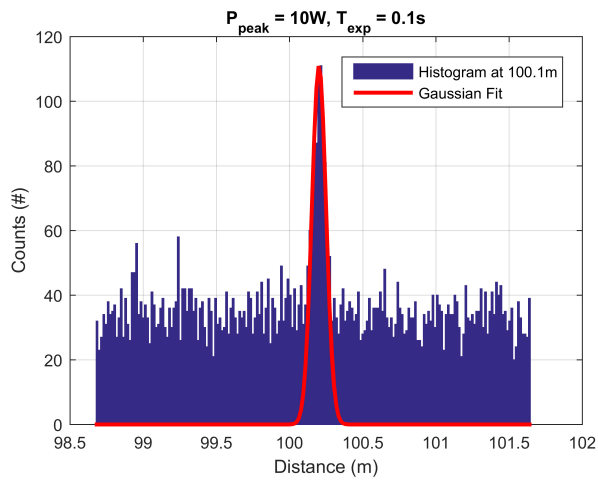


Figure 19. Simulated Histogram for 100 m Distant Target using the Gen2 System Parameters

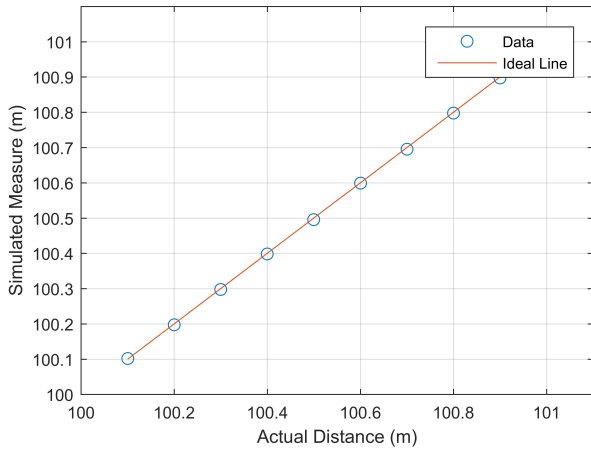


Figure 20. Ranging at 100 m, Using the Gen2 System Parameters in Table 5 and Giving <10 cm Resolution

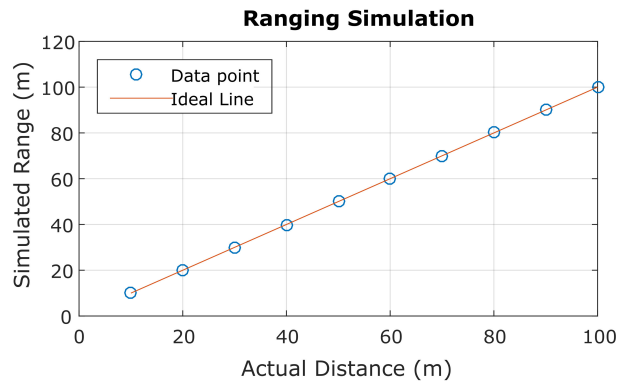


Figure 21. Simulated Ranging Data for 10 m up to 100 m using the Gen2 System Parameters and Showing Good Linearity

Table 6. SIMULATED PERFORMANCE OF THE GEN2 RANGING DEMONSTRATOR FOR RANGING TO 100 M (100 KLUX, AMBIENT LIGHT, LED, 150 KHZ).

| Long Range | |
|------------|--------|
| Range | 100 m |
| Accuracy | <10 cm |
| Resolution | <10 cm |

Further Help

1. [Ranging Demonstrator Description](#) – This document describes the specification and operation of the Ranging Demonstrator. This demonstrator is an engineering prototype. Its purpose is to demonstrate SiPM technology in ranging applications and to provide feedback for modelling of future designs.
2. [Introduction to SiPM](#) – This document introduces the basic concepts of the Silicon Photomultiplier for those who are new to this type of sensor.
3. [How to Evaluate and Compare SiPM Sensors](#) – This document discusses some of the primary factors to be considered in the selection of the optimum SiPM.
4. [C-Series Datasheet](#) – The datasheet for the sensors used in this document.

onsemi, **Onsemi**, and other names, marks, and brands are registered and/or common law trademarks of Semiconductor Components Industries, LLC dba "**onsemi**" or its affiliates and/or subsidiaries in the United States and/or other countries. **onsemi** owns the rights to a number of patents, trademarks, copyrights, trade secrets, and other intellectual property. A listing of **onsemi**'s product/patent coverage may be accessed at www.onsemi.com/site/pdf/Patent-Marking.pdf. **onsemi** reserves the right to make changes at any time to any products or information herein, without notice. The information herein is provided "as-is" and **onsemi** makes no warranty, representation or guarantee regarding the accuracy of the information, product features, availability, functionality, or suitability of its products for any particular purpose, nor does **onsemi** assume any liability arising out of the application or use of any product or circuit, and specifically disclaims any and all liability, including without limitation special, consequential or incidental damages. Buyer is responsible for its products and applications using **onsemi** products, including compliance with all laws, regulations and safety requirements or standards, regardless of any support or applications information provided by **onsemi**. "Typical" parameters which may be provided in **onsemi** data sheets and/or specifications can and do vary in different applications and actual performance may vary over time. All operating parameters, including "Typicals" must be validated for each customer application by customer's technical experts. **onsemi** does not convey any license under any of its intellectual property rights nor the rights of others. **onsemi** products are not designed, intended, or authorized for use as a critical component in life support systems or any FDA Class 3 medical devices or medical devices with a same or similar classification in a foreign jurisdiction or any devices intended for implantation in the human body. Should Buyer purchase or use **onsemi** products for any such unintended or unauthorized application, Buyer shall indemnify and hold **onsemi** and its officers, employees, subsidiaries, affiliates, and distributors harmless against all claims, costs, damages, and expenses, and reasonable attorney fees arising out of, directly or indirectly, any claim of personal injury or death associated with such unintended or unauthorized use, even if such claim alleges that **onsemi** was negligent regarding the design or manufacture of the part. **onsemi** is an Equal Opportunity/Affirmative Action Employer. This literature is subject to all applicable copyright laws and is not for resale in any manner.

PUBLICATION ORDERING INFORMATION

LITERATURE FULFILLMENT:
Email Requests to: orderlit@onsemi.com

onsemi Website: www.onsemi.com

TECHNICAL SUPPORT
North American Technical Support:
Voice Mail: 1 800-282-9855 Toll Free USA/Canada
Phone: 011 421 33 790 2910

Europe, Middle East and Africa Technical Support:
Phone: 00421 33 790 2910
For additional information, please contact your local Sales Representative